

CTRP9 Ameliorates Atrial Inflammation, Fibrosis, and Vulnerability to Atrial Fibrillation in Post-Myocardial Infarction Rats

Mingxin Liu, MD, PhD;* Wei Li, MS;* Huibo Wang, MD, PhD; Lin Yin, MS; Bingjie Ye, MS; Yanhong Tang, MD, PhD; Congxin Huang, MD, PhD*

Background—Inflammation and fibrosis play an important role in the pathogenesis of atrial fibrillation (AF) after myocardial infarction (MI). CTRP9 (C1q/tumor necrosis factor-related protein-9) as a secreted glycoprotein can reverse left ventricle remodeling post-MI, but its effects on MI-induced atrial inflammation, fibrosis, and associated AF are unknown.

Methods and Results—MI model rats received adenoviral supplementation of CTRP9 (Ad-CTRP9) by jugular-vein injection. Cardiac function, inflammatory, and fibrotic indexes and related signaling pathways, electrophysiological properties, and AF inducibility of atria in vivo and ex vivo were detected in 3 or 7 days after MI. shCTRP9 (short hairpin CTRP9) and shRNA were injected into rat and performed similar detection at day 5 or 10. Adverse atrial inflammation and fibrosis, cardiac dysfunction were induced in both MI and Ad-GFP (adenovirus-encoding green fluorescent protein)+MI rats. Systemic CTRP9 treatment improved cardiac dysfunction post-MI. CTRP9 markedly ameliorated macrophage infiltration and attenuated the inflammatory responses by downregulating interleukin-1 β and interleukin-6, and upregulating interleukin-10, in 3 days post-MI; depressed left atrial fibrosis by decreasing the expressions of collagen types I and III, α -SMA, and transforming growth factor β 1 in 7 days post-MI possibly through depressing the Toll-like receptor 4/nuclear factor- κ B and Smad2/3 signaling pathways. Electrophysiologic recordings showed that increased AF inducibility and duration, and prolongation of interatrial conduction time induced by MI were attenuated by CTRP9; moreover, CTRP9 was negatively correlated with interleukin-1 β and AF duration. Downregulation of CTRP9 aggravated atrial inflammation, fibrosis, susceptibility of AF and prolonged interatrial conduction time, without affecting cardiac function.

Conclusions—CTRP9 is effective at attenuating atrial inflammation and fibrosis, possibly via its inhibitory effects on the Toll-like receptor 4/nuclear factor- κ B and Smad2/3 signaling pathways, and may be an original upstream therapy for AF in early phase of MI. (*J Am Heart Assoc.* 2019;8:e013133. DOI: 10.1161/JAHA.119.013133.)

Key Words: atrial fibrillation • CTRP9 • fibrosis • inflammation • myocardial infarction

Atrial fibrillation (AF) is an increasingly common and serious healthcare problem that has shown to be related to increase in-hospital stays and mortality rates.¹ AF is the most common supraventricular rhythm interference following the arrhythmia complication of acute coronary syndrome

(ACS), with an estimated incidence of 6.8% to 21%, especially in ST-segment elevation acute myocardial infarction.^{2,3} Clinical research has prompted that there is a similar incidence of AF in the acute phase of MI compared with beyond 30 days after MI.⁴ The reason for new-onset AF in MI is multifactorial, including elevated left ventricular end-diastolic (LVED) pressure, deteriorated cardiac function, increased atrial overload, atrial ischemia, inflammation, oxidative stress, and neurohormonal activation of the sympathetic nervous system.^{5,6}

Increasing evidence approves the role of cardiac inflammation and consequential interstitial fibrosis as the pathophysiology of AF in the early phase of MI.^{7–9} Acute myocardial infarction leads to an intensive inflammatory response that is of utmost importance for the process of cardiac wound healing.¹⁰ Whereas the occurrence and persistence of AF has been shown to increase inflammation.^{7,11} Early inflammatory activation is an essential process for the transition to the later proliferative stage of interstitial fibrosis (3–7 days).^{12,13} Inflammation-mediated interstitial fibrosis, which leads to adverse atrial

From the Department of Cardiology, Renmin Hospital of Wuhan University, Hubei, China (M.L., W.L., H.W., L.Y., B.Y., Y.T., C.H.); Cardiovascular Research Institute of Wuhan University, Hubei, China (M.L., W.L., H.W., L.Y., B.Y., Y.T., C.H.); Hubei Key Laboratory of Cardiology, Hubei, China (M.L., W.L., H.W., L.Y., B.Y., Y.T., C.H.).

*Dr Liu and Dr Li contributed equally to this work.

Correspondence to: Congxin Huang, MD, PhD, Department of Cardiology, Renmin Hospital of Wuhan University, 238 Jiefang Road, Wuhan 430060, Hubei, China. E-mail: huangcongxin@vip.163.com

Received April 30, 2019; accepted September 18, 2019.

© 2019 The Authors. Published on behalf of the American Heart Association, Inc., by Wiley. This is an open access article under the terms of the Creative Commons Attribution-NonCommercial-NoDerivs License, which permits use and distribution in any medium, provided the original work is properly cited, the use is non-commercial and no modifications or adaptations are made.

Clinical Perspective

What Is New?

- CTRP9 (C1q/tumor necrosis factor-related protein-9) can reduce the occurrence of atrial fibrillation in the early stage of myocardial infarction by inhibiting the formation of atrial arrhythmogenic substrate, such as atrial fibrosis and inflammation, especially promoting macrophages polarization.

What Are the Clinical Implications?

- CTRP9 may act as a novel therapeutic target for the upstream prevention of atrial fibrillation in infarcted hearts.

remodeling, is one of the important mechanisms in the pathogenesis of AF. Thus, early and selective targeting therapy of injurious proinflammatory and fibrosis signals are conducive to decreasing the incidence of AF post-MI.

The CTRPs (C1q tumor necrosis factor [TNF]-related proteins) are a highly conserved family of adiponectin paralogs. Among the CTRPs, CTRP9 as a secreted glycoprotein is highly expressed in the heart.¹⁴ Some research studies found that CTRP9 expression in plasma and ventricular tissue is significantly reduced in ischemic, LPS-induced and high-fat diet-induced diabetic cardiac injury, inflammation may be a cause of CTRP9 reduction, and demonstrate that CTRP9 plays an important role in improving ventricular remodeling by suppressing inflammatory reactions and ameliorating cardiac fibrosis, partially related to the effects of CTRP9 on cardiomyocytes and macrophages.^{15–18} Excessive Toll-like receptor 4 (TLR4) and Smad2/3 activation, and increased expression of proinflammatory cytokines, such as interleukin-1 β (IL-1 β) and interleukin-6 (IL-6), and fibrosis mediators in the downstream of TLR4 and Smad2/3 signaling have been demonstrated in heart from humans and animal models with acute myocardial infarction.^{19,20} Meanwhile, CTRP9 can prevent activation of the TLR4-NF- κ B p65 pathway to inhibit a cholesterol-induced vascular smooth muscle cell phenotype switch.²¹ Based on these findings and evidences, whether CTRP9 can regulate atrial inflammatory responses and fibrosis in the early stage of post-MI by affecting TLR4 and Smad2/3 pathways remains unknown.

Therefore, the purpose of this study was to validate the hypothesis that CTRP9 may play a vital role in atrial remodeling and could depress atrial inflammatory and profibrotic properties and related signaling pathways, and decrease vulnerability to AF in a rat MI model.

Methods

The data that support the findings of this study are available from the corresponding author upon reasonable request.

Construction of Adenoviral Vector

Recombinant adenovirus (Ad)-encoding rat full-length CTRP9 (fCTRP9) gene (Ad-CTRP9, PubMed No. NM_001191891), or green fluorescent protein as a control transgene (Ad-GFP), were constructed and amplified. After confirming the sequence, we purified the recombinant replication-defective adenovirus and measured the final plaque-forming units (pfu) (Hanbio, Shanghai, China).

Adenovirus-mediated silencing of CTRP9 was performed as described previously.²² Brief, knockdown of CTRP9 was performed using adenoviral vectors carrying CTRP9 short hairpin RNAs (Ad-shCTRP9-GFP, shCTRP9), which were generated by Hanbio (Shanghai, China), scrambled shRNA-GFP (shRNA) was used as the control.

Animals and Ethics

All adult male Sprague-Dawley rats in vivo and ex vivo experiments (weighing 180–220 g) were purchased from the Animal Center of the Renmin Hospital of Wuhan University. This study conforms to the *Guide for the Care and Use of Laboratory Animals* published by the US National Institutes of Health (the Eighth Edition, National Research Council 2011). All specific pathogen-free animals were housed separately and were kept in a light-controlled environment with a 12-hour light/dark cycle, temperature and humidity control, and free access to standard rat food and water.

Experimental Protocol and Cardiac Function

The rat MI model was induced by ligating the left anterior descending coronary artery as previously described.²³ Evidence of MI was determined by ST segment elevation and the occurrence of Q wave on an ECG. All Sprague-Dawley rats were randomly divided into 4 groups: (1) sham; (2) MI; (3) Ad-GFP+MI; and (4) Ad-CTRP9 +MI. Then, the rats were given a jugular-vein injection of Ad-CTRP9 or Ad-GFP at a dose of 3×10^9 pfu per rat 5 days before MI. Rats were anesthetized with an intraperitoneal injection of 3% pentobarbital sodium (40 mg/kg). According to previously described procedures,²⁴ transthoracic echocardiography was performed at day 7, and the left ventricular end-diastolic diameter, left ventricular ejection fraction, and left ventricular fractional shortening were measured. The rats were euthanized by intracardiac injection of KCl to induce diastolic arrest of cardiac activity at 3 or 7 days post-MI.

shCTRP9 and shRNA were prepared, and we injected 2.5×10^{10} pfu of adenovirus into rats through the jugular vein. Rats were euthanized at day 5 or 10 after adenovirus injection.

Masson Trichrome Staining

Rat hearts were divided into atria and ventricles, and isolated left atria (LA) were fixed in 4% paraformaldehyde for 24 hours, embedded in paraffin, and sectioned transversely at 5 μ m. Masson trichrome staining was used to evaluate interstitial fibrosis. Images were visualized by light microscopy (ECLIPSE 80i; Nikon, Japan). The LA fibrotic area was analyzed at $\times 400$ magnification as the percentage of area of positive fibrotic staining divided by total myocardial tissue areas by using image analysis system software (Image-Pro Plus version 6.0).

Immunofluorescence Staining

Three atrial sections from each rat were incubated with individual primary antibodies to inducible nitric oxide synthase (iNOS) (1:500; Servicebio Technology, Wuhan, China) or CD163 (1/500; Abcam, Cambridge, MA) and CD68 (1:3000; Servicebio Technology, Wuhan, China), collagen I (1:500; Abcam) or collagen III (1:1000; Abcam) and α -actinin (1:100; Abcam) overnight at 4°C. Subsequently, secondary antibodies conjugated with fluorescein (FITC/CY3) were incubated for 1 hour at room temperature while avoiding light. The slides were washed 3 times with PBS, incubated in 4, 6-diamino-2-phenylindole (DAPI; 1:1; Servicebio Technology, Wuhan, China), and then dried and cover-slipped for evaluation. Fluorescent signals of 5 random non-overlapping fields were captured with a fluorescence microscope (Nikon Eclipse C1, Tokyo, Japan). All images were analyzed by Image-Pro Plus 6.0 software. Quantification of macrophages and collagen volume fraction (CVF) was calculated as the percentage of positively stained area to total area at $\times 400$ magnification.

Cytokine Quantification

Following treatment, cytokine CTRP9 (Baolai, Jiangsu, China) levels from plasma and IL-1 β (Elabscience, Wuhan, China)

levels in LA tissue were measured using rat ELISA kits according to the manufacturer's instructions. Protein levels were calculated from a cytokine standard curve. Tissue ELISA measurements were normalized to the protein content of the homogenates (pg/mg of proteins).

Real-Time Polymerase Chain Reaction Analysis

The real-time polymerase chain reaction (RT-PCR) procedure was performed as previously described.²⁵ Total RNA was extracted from atrial tissue using a Trizol (Invitrogen, Carlsbad, CA) as directed by the manufacturer. The RNA (2 μ g of each sample) was reverse-transcribed into cDNA using oligo (DT) primers, and single-stranded cDNA was transcribed with the help of the PrimeScript RT reagent Kit with gDNA Eraser (Takara, Dalian, China). Quantitative RT-PCR was performed using SYBR Premix Ex TaqII (TaKaRa) in StepOne Real-Time PCR detection System (Invitrogen). The transcript level was measured relative to that of GAPDH that was obtained from a standard curve. The primer sequences used are listed in Table.

Western Blot Analysis

Western blot analysis was performed as previously described.²⁵ Proteins were extracted from atrial tissue and resolved by SDS-PAGE (10% gels) and transferred to polyvinylidene difluoride (Millipore, Hong Kong, China) membranes. After blocking, the membranes were incubated with the following the primary antibodies: anti- α -SMA rabbit antibody (1:500; Abcam), anti-transforming growth factor β 1 rabbit antibody (1:1000; Abcam), anti-TLR4 rabbit antibody (1:1000; Affbiotech, Cincinnati, OH), anti-p-NF- κ B p65 (1:500; Abcam), anti-NF- κ B p65 rabbit antibody (1:3000; Abcam), anti-p-Smad2/3 (1:100; Abcam), anti-Smad2/3 (1:100; Abcam) rabbit antibody, and anti-GAPDH rabbit antibody

Table. Information of Primers for RT-PCR

Gene Name	Forward Sequence (5'-3')	Reverse Sequence (5'-3')
Rat-CTRP9	GGCTTCTACTGGTTATGGACGC	GGAGCCTGGATCACCTTTGAT
Rat-CD68	ACCCGGAGACGACAATCAAC	CTTGGTGGCCTACAGAGTGG
Rat-iNOS	AGCATCCACGCCAAGAACG	GTCTGGTTGCCTGGGAAAT
Rat-IL-1 β	GTGGCAGCTACCTATGTCTTGC	CCACTTGTGGCTTATGTTCTGT
Rat-IL-6	TGGAGTCCGTTTCTACCTGG	GGTCCTTAGCCACTCCTTCTGT
Rat-IL-10	TGCAACAGCTCAGCGCA	GTCACAGCTTTCGAGAGACTGGAA
Rat-Collagen I	CCGTGACCTCAAGATGTGCC	GAACCTTCGCTTCCATACTCG
Rat-Collagen III	GACCTCTGGAAAAGATGGATC	AAATCCATTGGATCATCCCC
Rat-GAPDH	CGCTAACATCAAATGGGGTG	TTGCTGACAATCTTGAGGGAG

CTRP9 indicates C1q/tumor necrosis factor-related protein-9; IL, interleukin; iNOS, inducible nitric oxide synthase.

(1:10000; Abcam). After washing, membranes were incubated with horseradish peroxidase-goat anti-rabbit-conjugated secondary antibodies (1:10000; ASPEN, Massachusetts, USA), and protein bands were visualized by enhanced chemiluminescence (ASPEN). The protein expression levels were normalized to GAPDH protein.

ECG Analysis

The rats were lightly anesthetized with isoflurane vapor (1.5% isoflurane in 98% O₂) and observed to sustain the lightest anesthesia. Three subcutaneous wires were positioned to simulate ECG limb lead II. ECG was recorded for 5 minutes, and ECG parameters (P wave duration, and PR interval) were measured 3 times as the average from these images that exceeded a 30-second interval at baseline reaching a steady state. The data were analyzed using LabChart 7 Pro (AD Instruments, Australia).²⁶

Electrophysiological Studies

All electrophysiological studies of atrium in *ex vivo* were tested according to previously reported methods.^{27,28} After 7 days of MI, hearts were isolated and perfused retrogradely using a Langendorff apparatus with HEPES-buffered Tyrode's solution (mM: NaCl 130; KCl 5.4; CaCl₂ 1.8; MgCl₂ 1; Na₂HPO₄ 0.3; HEPES 10; glucose 10; pH adjusted to 7.4 with NaOH) equilibrated with a 95% O₂ to 5% CO₂ gas mixture at 37.0°C and constant pressure of 60 mm Hg. Isolated hearts were stabilized for 10 minutes by perfusion at a constant flow rate before programmed electrical stimulation. Teflon-coated (except at their tips) silver bipolar electrodes were placed on the right atria (RA) appendage, LA appendage, and LV. The inter-electrode distance between the RA and LA was set at 10 mm to measure the interatrial conduction time (IACT) during right atrial pacing. The left and right atrial effective refractory periods (AERPs) were measured by the S2 extrastimulus method using 8 regularly paced beats with cycle lengths of 150, 120, and 90 ms. Burst RA pacing (cycle lengths of 50 ms, pulse duration of 10 ms) for 3 seconds with twice the threshold voltage was used to test for AF vulnerability in all groups of rats. AF was defined as a rapid irregular atrial rhythm with irregular R-R intervals lasting at least 1 second. The duration of AF was measured from the end of burst pacing to the first P wave detected after the rapid irregular atrial rhythm.

Statistical Analysis

Statistical analysis was performed using SPSS 22.0 or GraphPad Prism 5.01 software. Continuous data were evaluated for normality using the Shapiro-Wilk test. One-way ANOVA followed by the Bonferroni-Dunn test was used for

multiple comparisons of normally distributed data expressed as mean±SEM, and the Kruskal-Wallis test was used for non-repeated measures of non-normally distributed variables. Moreover, a student independent t-test was conducted to compare results between the 2 groups. AF incidence across groups was expressed as percentages and analyzed using the Fisher exact test. Pearson (normally distributed data) or Spearman (non-normally distributed data) correlation analysis was used to determine the relationship between the levels of plasma CTRP9 and LA tissue IL-1β and AF duration. A value of *P*<0.05 was considered significant.

Results

Adenoviral Supplementation of CTRP9 Ameliorates Cardiac Function Following MI

Because cardiac function is related to new-onset AF following acute myocardial infarction, we evaluated whether overproduction of CTRP9 attenuates MI-mediated LV dysfunction. As shown in Figure 1A, rats were systemically treated with Ad-CTRP9 or Ad-GFP via jugular-vein injection before the MI model operation. Adenoviral production of CTRP9 was markedly increased in plasma levels of CTRP9 at 3 and 7 days after MI compared with Ad-GFP-treated MI rats. Meanwhile, we measured the expression of CTRP9 mRNA levels in atrial and ventricular tissue after MI. Compared with the sham group, we found that CTRP9 gene expression was significantly downregulated in the MI and Ad-GFP+MI groups, and CTRP9 was markedly increased in the Ad-CTRP9-treated MI group (Figure 1B and 1C). Among the echocardiographic parameters, larger left ventricular end-diastolic diameter, and reduced EF and FS were observed in the MI and Ad-GFP group compared with the sham group, but MI rats receiving Ad-CTRP9 had improved the adverse effects at 7 days after MI (Figure 1E through 1G).

Changes of Atrial Macrophage Infiltration and Inflammatory Responses at 3 Days or 7 Days Post-MI

As presented in Figure 2A, cells expressing macrophage CD68 marker in the atrium were barely detectable after sham surgery, and increased at day 3 and 7 post-MI, but CD68-positive (CD68⁺) cells were more abundant at day 3 post-MI than at day 7. Similar results were obtained by detecting the mRNA levels of macrophage markers (CD68, iNOS) and inflammatory cytokines (IL-1β, IL-6, and IL-10), we found that except for IL-6 and IL-10, the mRNA levels of other indexes were higher at day 3 post-MI than at day 7 (Figure 2B and 2C). The results showed that atrial inflammation was more significant at day 3 post-MI than at day 7.

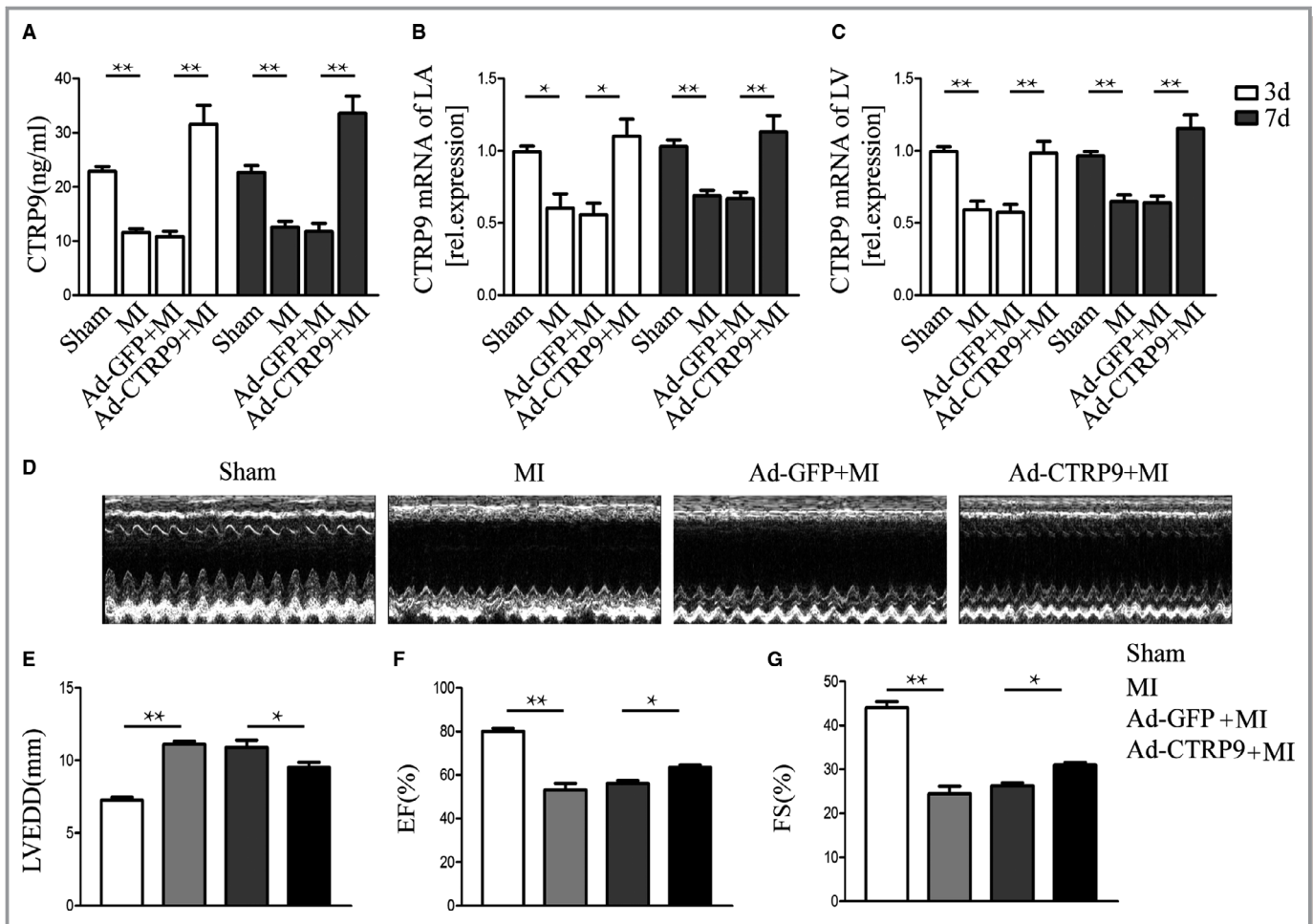


Figure 1. CTRP9 improves cardiac function on day 7 post-myocardial infarction. Ad-CTRP9 or Ad-GFP was injected into the jugular vein of rats 5 days before myocardial infarction. **A**, Effects of adenoviral CTRP9 supplement on plasma CTRP9 level by ELISA kit analysis (n=7 per group). **B** and **C**, CTRP9 mRNA levels were determined in left atria and left ventricle tissue of rats by real-time polymerase chain reaction methods (n=4 per group). **D**, Representative M-mode echocardiograms for rats in 7 days. **E** through **G**, Quantitative analysis of echocardiography evaluated LV function in 7 days (n=7 per group). The data are expressed as mean±SEM. * $P<0.05$, ** $P<0.01$, the connection represents a comparison between the 2 groups. Ad-CTRP9 indicates adenoviral CTRP9 constitutively overexpression; CTRP9, C1q/TNF-related protein-9; EF, ejection fraction; FS, fractional shortening; GFP, green fluorescent protein; LA, left atria; LV, left ventricle; LVEDD, left ventricular end-diastolic diameter; MI, myocardial infarction.

CTRP9 Promotes M2 Macrophage Polarization in the LA After MI

Inflammation is involved in the formation of AF. The inflammation level after MI is related to the time progression. According to the results of Figure 2, we observed the effect of CTRP9 on atrial inflammation at 3 days post-MI, instead of the effect at 7 days post-MI. To clarify the effect of CTRP9 on macrophage infiltration and M1 to M2 macrophage polarization transition, immunostaining was performed to assess macrophage infiltration by quantifying the percentage of CD68-positive (CD68⁺) macrophages in the LA at 3 days post-MI; meanwhile, to identify the subtype of infiltrated macrophages in the atrium, the markers for M1 (iNOS⁺/CD68⁺) and M2 (CD163⁺/CD68⁺) were examined.²⁹ We found that CD68⁺

and iNOS⁺/CD68⁺ macrophages were increased from the MI and Ad-GFP groups compared with the sham group, whereas there was no significant difference in the slightly increased proportion of CD163⁺/CD68⁺ at 3 days post-MI compared with the sham group. CTRP9 treatment significantly reduced the accumulation of CD68⁺ cells and the transition of M1 macrophages and promoted M2 polarization by upregulating the percentage of CD163⁺/CD68⁺ after MI (Figure 3A and 3B). Similar results were obtained for quantitative analysis of mRNA expression of CD68, iNOS and CD163 (Figure 3C through 3E). The upregulation of IL-1 β and IL-6 mRNA were seen in the atria of vehicle-treated MI and Ad-GFP-treated MI rats at day 3 after MI, IL-10 slightly increased in the 2 groups, but there was no significant difference, CTRP9 can inhibit the upregulation of IL-1 β and IL-6 and increase the expression of

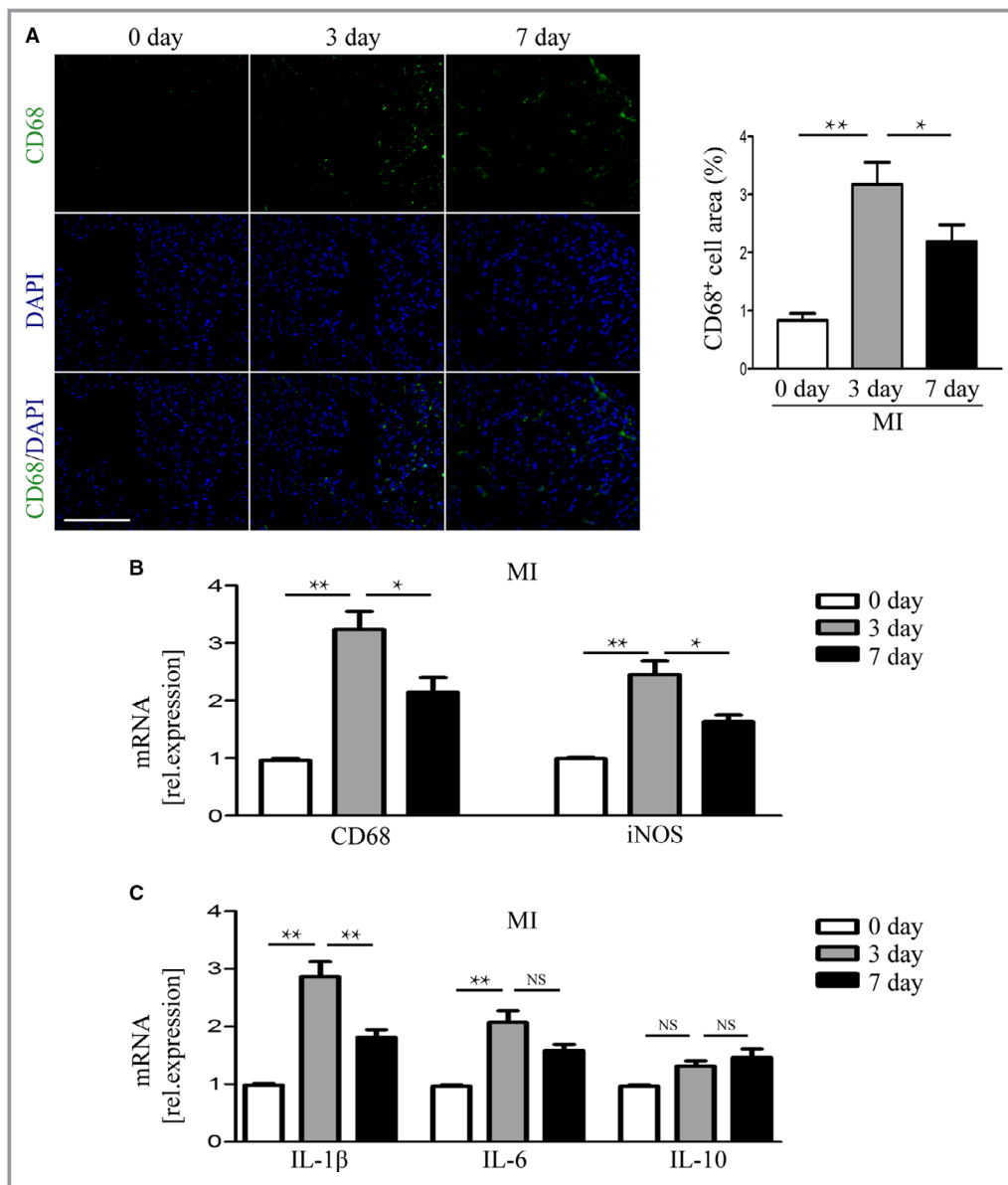


Figure 2. Comparison of inflammatory response in the atrium at 3 and 7 days post-myocardial infarction. **A**, Representative fluorescent immunostaining images. Left atria at 0, 3, and 7 days after myocardial infarction were stained with anti-CD68 antibody (green) and DAPI (blue). ($\times 400$ magnification, scale bar: 20 μm). Quantitative analysis of CD68⁺ macrophage area. **B** and **C**, quantitative real-time polymerase chain reaction analysis of mRNA change of CD68, inducible nitric oxide synthase, IL-1 β , IL-6, and IL-10. The data are expressed as the mean \pm SEM (n=4 per group). NS>0.05, * P <0.05, ** P <0.01, the connection represents a comparison between the 2 groups. iNOS, inducible nitric oxide synthase; DAPI, 4,6-diamino-2-phenylindole; IL, interleukin.

IL-10 (Figure 3F through 3H). CTRP9 administration partially inhibited atrial proinflammatory response by promoting M1 to M2 macrophage polarization after MI.

CTRP9 Inhibits LA Interstitial Fibrosis Post-MI

To investigate the effect of CTRP9 on AF to AF substrate formation at 7 days after MI, the production and deposition of

collagen, and the differentiation of cardiac fibroblasts to myofibroblasts, were estimated using Masson trichrome staining, collagen immunofluorescence staining, RT-PCR, western blot analysis. The Masson trichrome-stained sections identified that MI increased fibrosis-positive areas in the LA, and CTRP9 decreased the fibrotic areas post-MI (Figure 4A and 4D). As indicated by immunofluorescent staining (Figure 4B and 4E; 4C and 4F), MI increased the deposition of collagen I and III types,

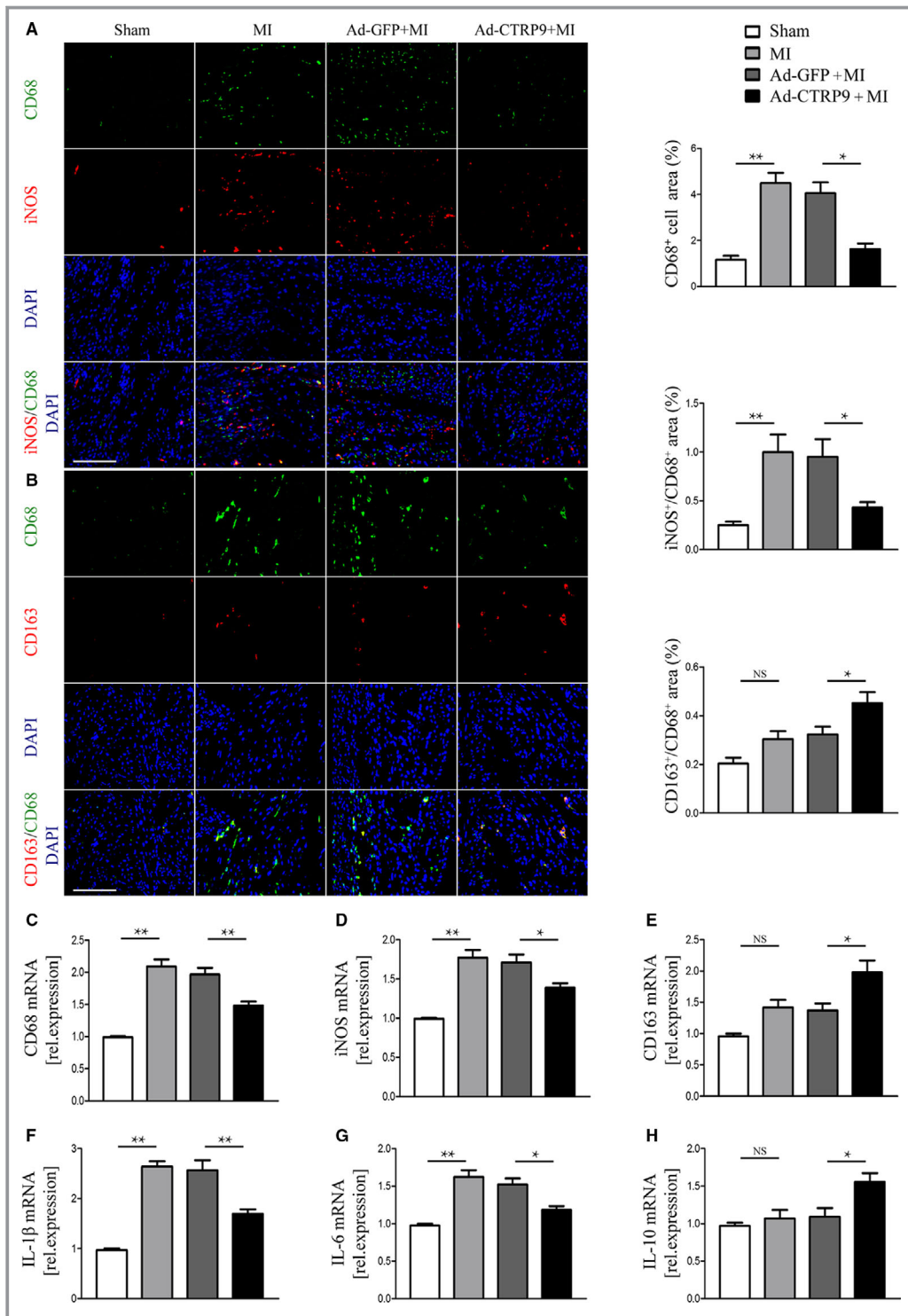


Figure 3. Anti-inflammatory effects of CTRP9 on myocardial infarction injury. **A** and **B**, Representative fluorescent immunostaining images. Left atria at 3 days after myocardial infarction were stained with anti-CD68 antibody (green), anti-inducible nitric oxide synthase and CD163 antibody (red), and DAPI (blue). Scale bar: 20 μ m. Quantitative analysis of the area of infiltrating CD68-positive and inducible nitric oxide synthase (iNOS)-negative cells (CD68⁺) macrophages in left atria. Quantitative assessment of iNOS⁺ or CD163-positive and CD68-positive (iNOS⁺/CD68⁺, CD163⁺/CD68⁺) area of cells (right column). (n=4 per group). **C** through **H**, Expression of CD68, inducible nitric oxide synthase, CD163, interleukin-1 β , interleukin-6, and interleukin-10 mRNA in left atria, respectively (n=4 per group). The data are expressed as the mean \pm SEM. NS, $P>0.05$, * $P<0.05$, ** $P<0.01$, the connection represents a comparison between the 2 groups.

and CTRP9 treatment significantly reduced these productions. Consistent effect of CTRP9 on gene expression of collagen I and III was also demonstrated through RT-PCR analysis (Figure 4I and 4J). Considering that previous studies have suggested that the ratio of type I CVF to type III CVF (CVF I/III ratio) is closely related with AF duration,³⁰ we evaluated the correlation between CVF I/III ratio and AF duration, a significant positive correlation was evident (Spearman $r=0.714$, $P=0.047$; Figure 4G), but it was further observed that CTRP9 had no effect on CVF I/III ratio (Figure 4H). The expressions of α -smooth muscle actin (α -SMA), a marker for over-proliferation of myofibroblasts, and transforming growth factor β 1 (TGF- β 1) were found to be significantly higher in the MI and Ad-GFP+MI groups than those in the sham group and markedly lower in the Ad-CTRP9+MI group using western blot analysis (Figure 4K and 4L).

Effects of CTRP9 on Atrial Electrophysiology and AF Inducibility

Figure 5A shows representative examples ECG, LA, and LV electrogram traces in a rat with induced AF through atrial burst pacing ex vivo using isolated perfused hearts at 7 days after MI. After termination of the burst, the irregular atrial rhythm with irregular ventricular response was presented as a typical electrogram of AF. As shown in Figure 5B, RA burst-stimuli transiently induced AF in 8.3% (1 of 12) of animals in the sham group. MI aggravated the vulnerability to AF, and the results showed induced AF in 7 of 12 (58.3%) of MI and 8 of 12 (66.6%) of Ad-GFP+MI rats that was suppressed by CTRP9 administration (2 of 10, 20%). Average AF duration was longer in the MI and Ad-GFP+MI groups than those in the sham group (28.10 ± 15.05 s, 30.21 ± 13.69 s versus 0.31 ± 0.31 s). CTRP9 administration shortened AF duration (1.05 ± 0.73 s) (Figure 5C).

In addition, there were no differences between the 4 groups in the duration of P wave (Figure 5D). The PR interval was increased significantly in MI and Ad-GFP+MI groups compared with the sham group; however, CTRP9 markedly reduced the PR interval (Figure 5E). In addition, compared with the sham group, IACT in the MI and Ad-GFP groups was prolonged at all the basic cycle lengths tested, and MI-induced prolongation of IACT was attenuated by CTRP9 administration (Figure 5F). The AERP of the LA or RA at any of the basic cycle lengths tested was significantly longer in MI and Ad-GFP rats compared with the sham rats. No significant differences in AERP were observed among Ad-GFP and Ad-CTRP9 groups; notwithstanding, ERP in the Ad-CTRP9 group had a shortened trend (Figures 5G and 5H).

The atrial levels of IL-1 β were significantly and positively correlated with AF duration (Spearman $r=0.93$, $P<0.001$; Figure 5I), and negatively correlated with CTRP9 (Pearson $r=0.79$, $P<0.001$; Figures 5J); the plasma levels of CTR9 were

negatively correlated with AF duration (Spearman $r=0.86$, $P<0.001$; Figure 5K).

Down-Regulation of CTRP9 Deteriorates Atrial Inflammation and Fibrosis, Without Affecting LV Cardiac Function

To obtain more evidence to support our hypothesis, we knocked down CTRP9 by adenovirus mediated shCTRP9 in rat. The plasma and atrial CTRP9 levels after shCTRP9 delivery were evaluated quantitatively by Elisa and by PCR analysis. The results were shown in Figure 6A and 6B. Treatment with shCTRP9 but not shRNA significantly decreased the expression of CTRP9 at day 10 after shCTRP9 injection in rat. Reduced CTRP9 did not cause significant LV cardiac dysfunction (Figure 6C through 6E). As expected, silencing of CTRP9 induced atrial inflammation, the atrial CD68⁺ and iNOS⁺/CD68⁺ ratio was significantly higher in shCTRP9 rat than shRNA rat (Figure 6F through 6H), moreover, shCTRP9 resulted in significantly higher elevations of CD68, iNOS, IL-1 β and IL-6 mRNA levels (Figure 6I through 6J). Atrial sections stained by Masson trichrome staining shown that downregulation of CTRP9 lead to interstitial fibrosis (Figure 6K through 6L); the mRNA levels relating to cardiac fibrosis, collagen I and III and TGF- β 1, were significantly higher in shCTRP9 rat than shRNA rat, there was no apparent difference of α -SMA under silencing CTRP9 (Figure 6M).

Silencing CTRP9 Aggravates Occurrence of AF and Prolongs IACT

AF can be significantly induced after 10 days of shCTRP9 treatment, there was more induction of AF in shCTRP9 group (8/11, 72.3%) compared with shRNA group (2/10, 20%) (Figure 7A and 7B). AF duration was also significantly increased in shCTRP9 rats (17.30 ± 7.74 s versus 0.85 ± 0.57 s) (Figure 7C). IACT was significantly longer in shCTRP9 group (Figure 7D). However, there was no significant differences in ERP of LA between the 2 groups (Figure 7E).

Effects of CTRP9 on Expression of Atrial Inflammatory and Fibrosis Protein Markers of Signaling Pathways

To explore the molecular mechanisms underlying the protective action of CTRP9 for atrial inflammation and fibrosis, we assessed the levels of TLR4/NF- κ B and Smad2/3 that were critical in the pathogenesis of atrial inflammation and fibrosis. As shown in Figure 8A through 8C, compared with the sham group, the expression of TLR4, phospho-NF- κ B p65/NF- κ B p65, and phospho-Smad2/3/Smad2/3 was upregulated in the MI and Ad-GFP groups, respectively. However, CTRP9

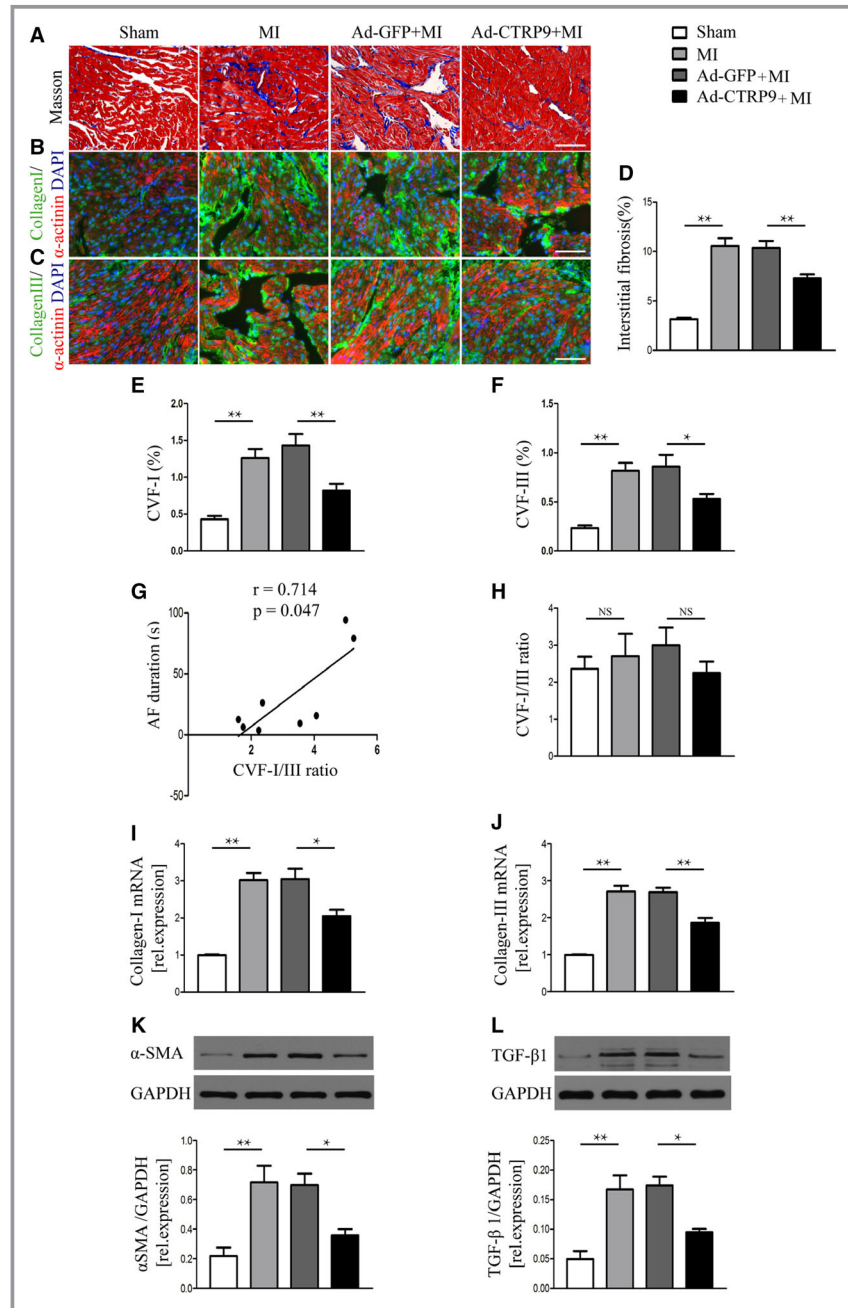


Figure 4. Therapeutic effects of CTRP9 on left atrial interstitial fibrosis post-myocardial infarction. **A** through **C**, Representative images of left atrial tissues at 7 day post-myocardial infarction stained with Masson trichrome staining, collagen I or collagen III (green)/ α -actinin (red) immunofluorescence staining. Scale bar: 50 μ m. **D** through **F**, Quantitative analysis of fibrosis, type I and III collagen volume fraction. Correlation between collagen volume fraction-I/III ratio with AF duration (**G**) and collagen volume fraction-I/III ratio levels comparison (**H**). **I** and **J**, The mRNA levels of collagen I and collagen III were examined by real-time polymerase chain reaction. **K** and **L**, The protein levels of α SMA and transforming growth factor- β 1 were measured by western blot analysis. The data are expressed as the mean \pm SEM (n=4 per group). * P <0.05, ** P <0.01, the connection represents a comparison between the 2 groups. ASMA indicates α smooth muscle actin; CVF, collagen volume fraction; MI, myocardial infarction; TGF- β 1, transforming growth factor- β 1.

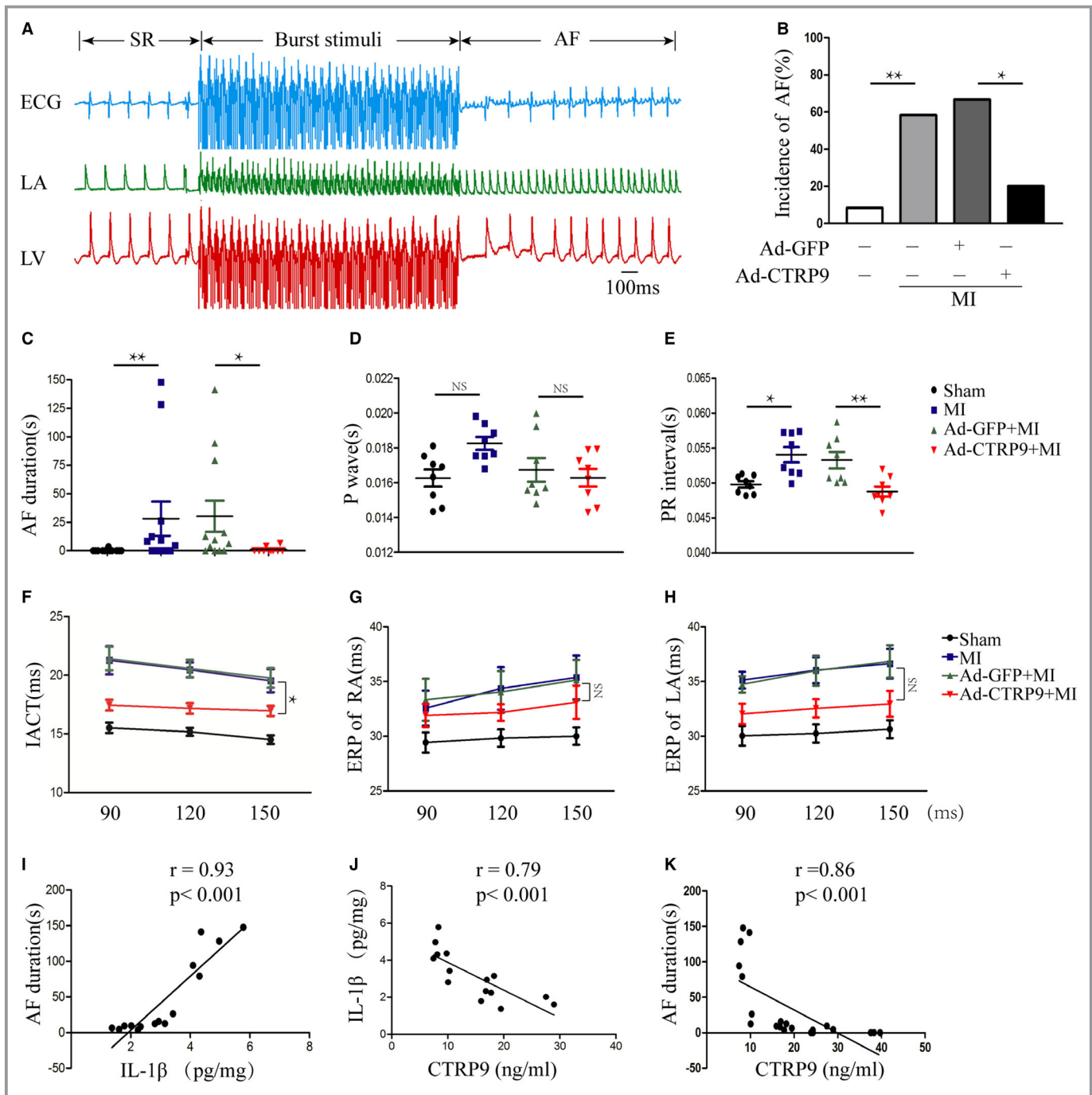


Figure 5. Recordings of atrial electrophysiological characteristics post-myocardial infarction under CTRP9 intervention. **A**, Representative atrial fibrillation episodes after atrial burst pacing observed in isolated perfused heart at 7 day post-myocardial infarction. **B** and **C**, Inducibility of atrial fibrillation and atrial fibrillation duration ($n=12, 12, 12, 10$ per group, correspondingly). **D** and **E**, The duration of P-wave and PR interval from in vivo ECG were analyzed ($n=8$ per group). **F** through **H**, Interatrial conduction time and ERP of the right atria and left atria were measured at basic cycle lengths of 150, 120, and 90 ms ($n=7$ per group). **I** and **J**, The relationship between interleukin-1 β and atrial fibrillation duration, CTRP9 is shown ($n=15$). **K**, The relationship between CTRP9 and AF duration is shown ($n=21$). NS, $P>0.05$, * $P<0.05$, ** $P<0.01$, the connection represents a comparison between the 2 groups. Ad-CTRP9 indicates adenoviral C1q/TNF-related protein-9 constitutively overexpression; Ad-GFP, adenovirus-encoding green fluorescent protein; AF, atrial fibrillation; BCL, basic cycle lengths; ERP, effective refractory period; IACT, interatrial conduction time; LA, left atria; LV, left ventricle; MI, myocardial infarction; PR interval, the time interval from beginning of the P-wave to the beginning of the R-wave; SR, sinus rhythm.

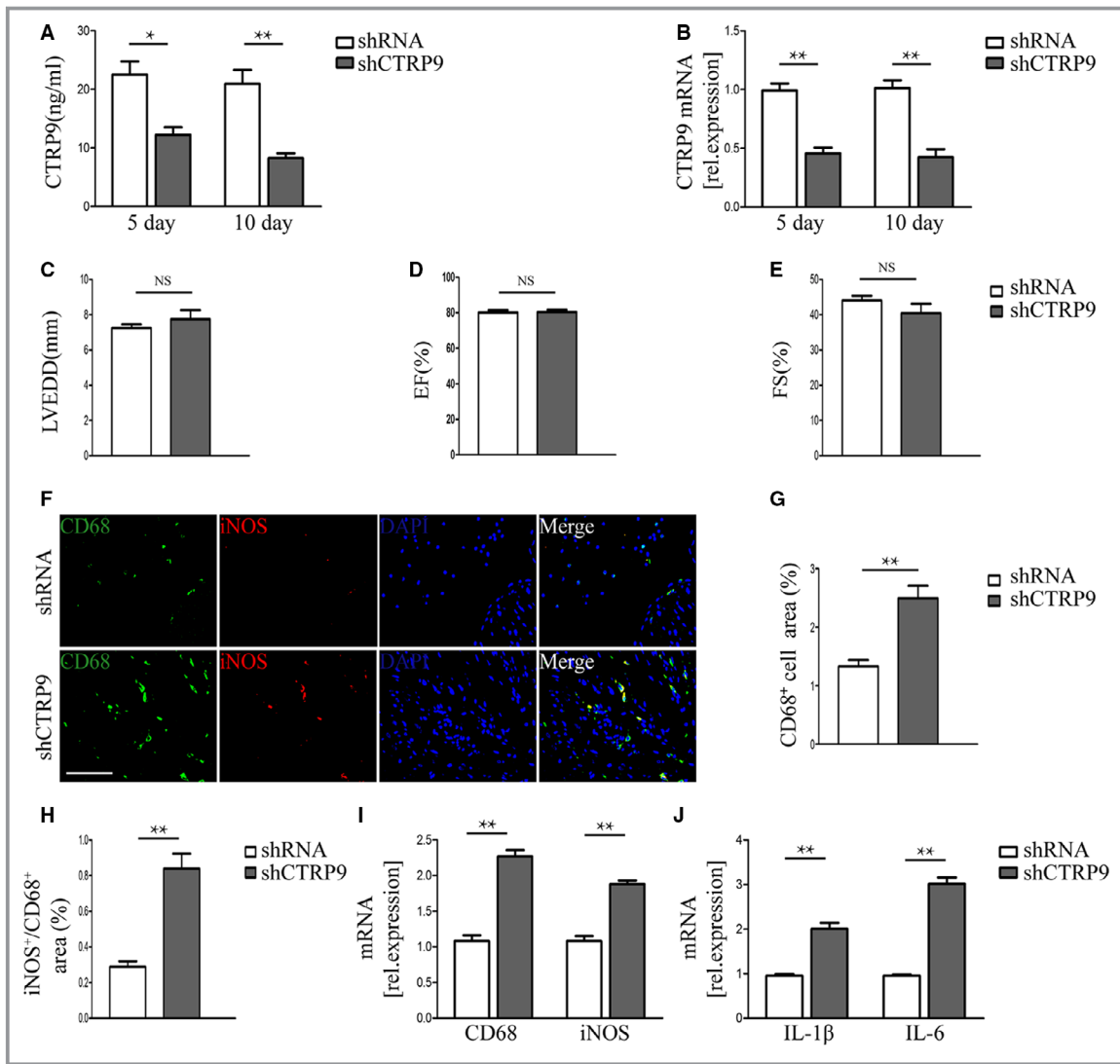


Figure 6. Effects of Ad-shCTRP9 on cardiac function, atrial inflammation, and fibrosis. Ad-shCTRP9 (shCTRP9) or Ad-shRNA (shRNA) was injected into the jugular vein of rats. Alteration of plasma CTRP9 levels by ELISA kit analysis (A) and atrial CTRP9 mRNA levels by real-time polymerase chain reaction methods (B) at day 5 or 10 after shCTRP9 injection. C through E, Quantitative analysis of echocardiography evaluated LV function at day 10 after shCTRP9 treatment. F, Representative fluorescent immunostaining images. Left atria at day 10 after shCTRP9 treatment were stained with CD68 (green), inducible nitric oxide synthase (red), and DAPI (blue). Scale bar: 20 μ m. Quantitative analysis of the area of infiltrating CD68⁺ (G) and iNOS⁺/CD68⁺ (H) macrophages in left atria. I and J, Expression of CD68, inducible nitric oxide synthase, interleukin-1 β and interleukin-6 mRNA in left atria. K, Representative images stained with Masson trichrome staining. Scale bar: 50 μ m. L, Quantitative analysis of atrial fibrosis at day 10 after shCTRP9 treatment. M, The mRNA levels of collagen I, collagen III, α -SMA and transforming growth factor- β 1 were detected by real-time polymerase chain reaction. The data are expressed as the mean \pm SEM (n=4 per group). NS, $P>0.05$, * $P<0.05$, ** $P<0.01$, the connection represents a comparison between the 2 groups. shCTRP9, CTRP9 short hairpin RNAs; shRNA indicates control group.

treatment notably suppressed the expression and activation of these proteins. To understand further role of CTRP9 in atrial inflammation and fibrosis, we tested these markers in the shRNA and shCTRP9-treated rat. Partial silencing of CTRP9 can significantly increase the expression of TLR4 and p-NF- κ B p65/NF- κ B p65 in rat atrium (Figure 8D and 8E), whereas such upregulation of p-Smad2/3/Smad2/3 was not observed in shCTRP9-treated rats (Figure 8F).

Discussion

In the present study, we provided the first direct evidence to demonstrate the potential protective role of CTRP9 in the pathogenesis of atrial inflammation, fibrosis, and AF in the early phase after MI. Our results confirmed that CTRP9 overexpression ameliorated cardiac LV function and the arrhythmogenic substrate in atria by partially reversing inflammation, especially the infiltration of macrophages, and

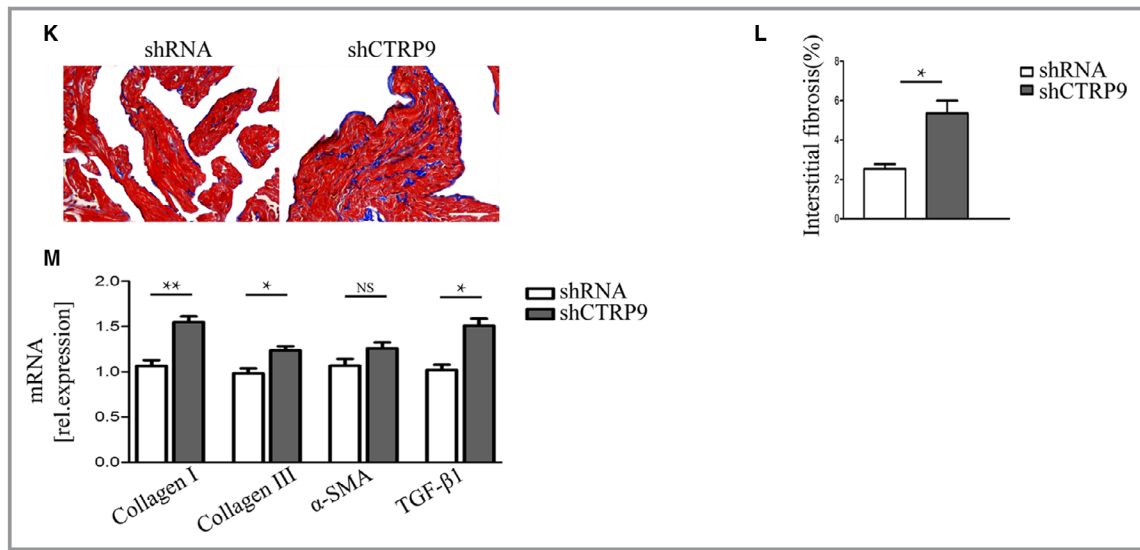


Figure 6. Continued.

fibrosis possibly by inhibiting the TLR4/NF- κ B and Smad2/3 signaling pathways, meanwhile, reduced susceptibility to AF and the atrial conduction function in rat MI models. Conversely, silencing CTRP9 in normal rats aggravated these effects, without affecting the cardiac function. These results point to the involvement of CTRP9 in the pathogenesis of atrial inflammation, fibrosis and AF, and suggest that CTRP9 will be a prospective therapeutic target for the upstream prevention of AF in post-MI hearts.

AF is an increasingly widespread healthcare problem that produces many hazards, primarily adverse cardiovascular and cerebrovascular events. Particularly, the occurrence of AF is easier to further impair ventricular function and coronary perfusion in the early stage of acute myocardial infarction.³ Therefore, we chose the early stage of MI disease model in the present study. Deterioration of cardiac function after MI is a cause of AF. Previous studies have shown that CTRP9 decreasing in post-MI attenuates LV remodeling and inhibits the inflammatory reactions following MI and pathological stimuli.^{15,16} Consistent with these data, our study shows that atrial and ventricular CTRP9 levels also appeared to decrease in 3-day and 7-day post-MI. Adenoviral supplementation of CTRP9 restoring or increasing CTRP9 levels of the circulatory system and heart was beneficial for the prevention of LV cardiac dysfunction. Here, considering that there was no significant change of left atrial diameter (LAD) at 7 day after MI,^{31–33} we did not detect the effect of CTRP9 on the LAD. In addition, we evaluated that effective downregulation of CTRP9 did not affect LV function of non-MI normal rats.

Atrial inflammation and fibrosis have emerged as important pathogenic contributors to AF recurrence by altering electrophysiological and structure remodeling, including disordered calcium handling, potassium current abnormality, conduction

heterogeneity, apoptosis, and atrial dilatation.^{13,34,35} Targeting the post-MI inflammation or fibrosis of the reparative phase at the onset might represent an effective anti-arrhythmic approach. The inflammatory response that accompanies the rapid influx of neutrophils and monocytes is primarily induced in the ventricles. The inflammatory response begins within hours after MI and peaks at 3 days post-MI. The predominant inflammatory cells are monocyte-derived macrophages in the phase, whereas proinflammatory M1 macrophages are the major subtypes. Secreted proinflammatory cytokines, including IL1 β and IL-6, are related to systemic inflammation and affect the atrial inflammation after MI that creates the substrate for arrhythmia.^{34,36,37} The peak time of atrial and ventricular inflammation is roughly similar at 3 days post-MI.^{37–39} The current results showed that the proinflammatory cytokines and total number of macrophages infiltrating the LA was markedly higher at day-3 than day-7 post-MI. MI induced the production and recruitment of M1 macrophages, releasing IL-1 β and IL-6 and aggravating cardiac function.^{29,40} IL-10 secreted by M2 macrophages can ameliorate adverse LV remodeling and inflammation post-MI.^{41,42} Moreover, previous studies also have confirmed that promoting M1 to M2 polarization can inhibit cardiac inflammation, fibrosis, and arrhythmias.^{43–45} Together with our findings, we considered that the analogous benefit of CTRP9 on atrium may be related with the promotion of M2 macrophage polarization. However, silencing CTRP9 can promote atrial inflammation, these results are consistent with the previous observations that CTRP9-knockout leads to inflammatory response in the LV myocardia.¹⁵

The activated TLR4/NF- κ B signaling pathway is involved in the increased M1 macrophage polarization and proinflammatory responses after MI, and acute myocardial infarction patients with new-onset AF have higher TLR4 expression in

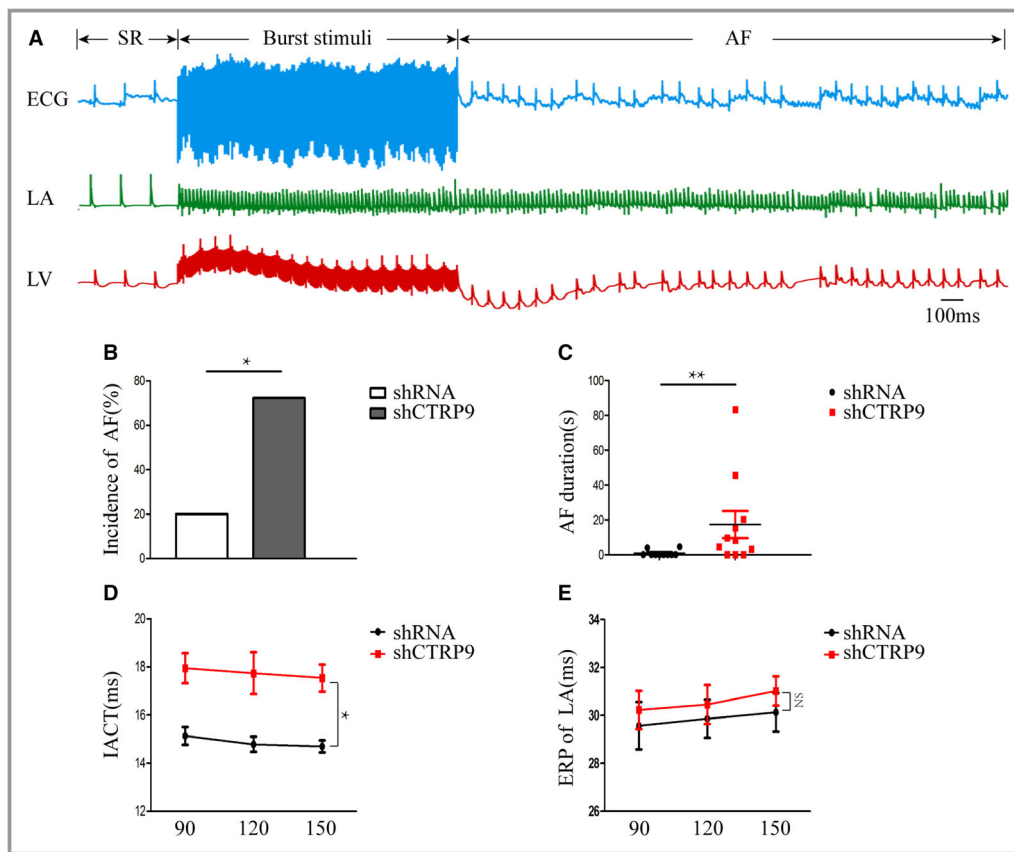


Figure 7. Silencing CTRP9 alters electrophysiological properties of atrium. **A**, Representative atrial fibrillation episodes after atrial burst pacing observed in isolated perfused heart at day 10 after shCTRP9 treatment. **B** and **C**, Inducibility of atrial fibrillation and trial fibrillation duration ($n=10, 11$ per group). **D** and **E**, interatrial conduction time and effective refractory period of the left atria were measured at basic cycle lengths of 150, 120, and 90 ms ($n=8$ per group). NS, $P>0.05$, * $P<0.05$, ** $P<0.01$, the connection represents a comparison between the 2 groups. AF indicates atrial fibrillation; IACT, interatrial conduction time; LA, left atrial; LV, left ventricle; shCTRP9 indicates CTRP9 small hairpin RNAs; shRNA, control group.

peripheral blood mononuclear cells,^{46–48} combined with the anti-inflammatory effect of CTRP9 and its effect on the TLR4/NF- κ B pathway.^{15,21} We found that MI also induced the levels of TLR4 elevation and NF- κ B p65 phosphorylation, whereas CTRP9 overexpression could reverse these changes. Furthermore, considering adiponectin, as a paralog of CTRP family, can reduce the expression of TLR4 in inflammatory cells by binding TLR4 promoter.⁴⁹ Hence, partial silencing CTRP9 upregulate the expression of TLR4 and NF- κ B p65 phosphorylation, which may be related with the dissociation of TLR4 promoter, but further verification needed. These results suggest that inhibiting the TLR4/NF κ B signaling pathway is involved in the anti-inflammatory effects of CTRP9.

Inflammation is considered to promote the consequential formation of atrial fibrosis in various models, and in turn recruit and activate reparative myofibroblasts, contributing to collagen synthesis and the progress of interstitial fibrosis.^{50–52} Meanwhile, many fibrogenic factors also can cause cardiac fibrosis.¹³ Therein, TGF- β 1 is a central cytokine in post-MI

atrial interstitial fibrosis formation to enhance the accumulation of the extracellular matrix and induce the differentiation of fibroblasts into myofibroblasts by activating Smad2/3 signals.^{19,34,53,54} Atrial fibrosis is an important pathogenesis of AF, especially with respect to electrical conduction disturbance, and fibroblast ion channels abnormality involving in Ca²⁺ entry pathways, inward rectifier K⁺ currents. These increase the heterogeneity of impulse propagation and enhance atrial re-entry, which may be directly related to the mechanisms responsible for initiating and maintaining AF.^{13,55,56} In the present study, CTRP9 markedly reduced fibrotic areas, deposition of collagen I/III type, and production of α SMA and TGF- β 1 of the LA at 7 day after MI. However, CTRP9 had no significant effect on CVF I/III ratio, which may be inconsistent with previous studies in the type and course of AF,³⁰ and speculated that atrial fibrosis evaluated by collagen in the early stage of MI may be involved in the occurrence of AF in this study, and CVF I/III ratio may have a greater influence on the maintenance and recurrence of

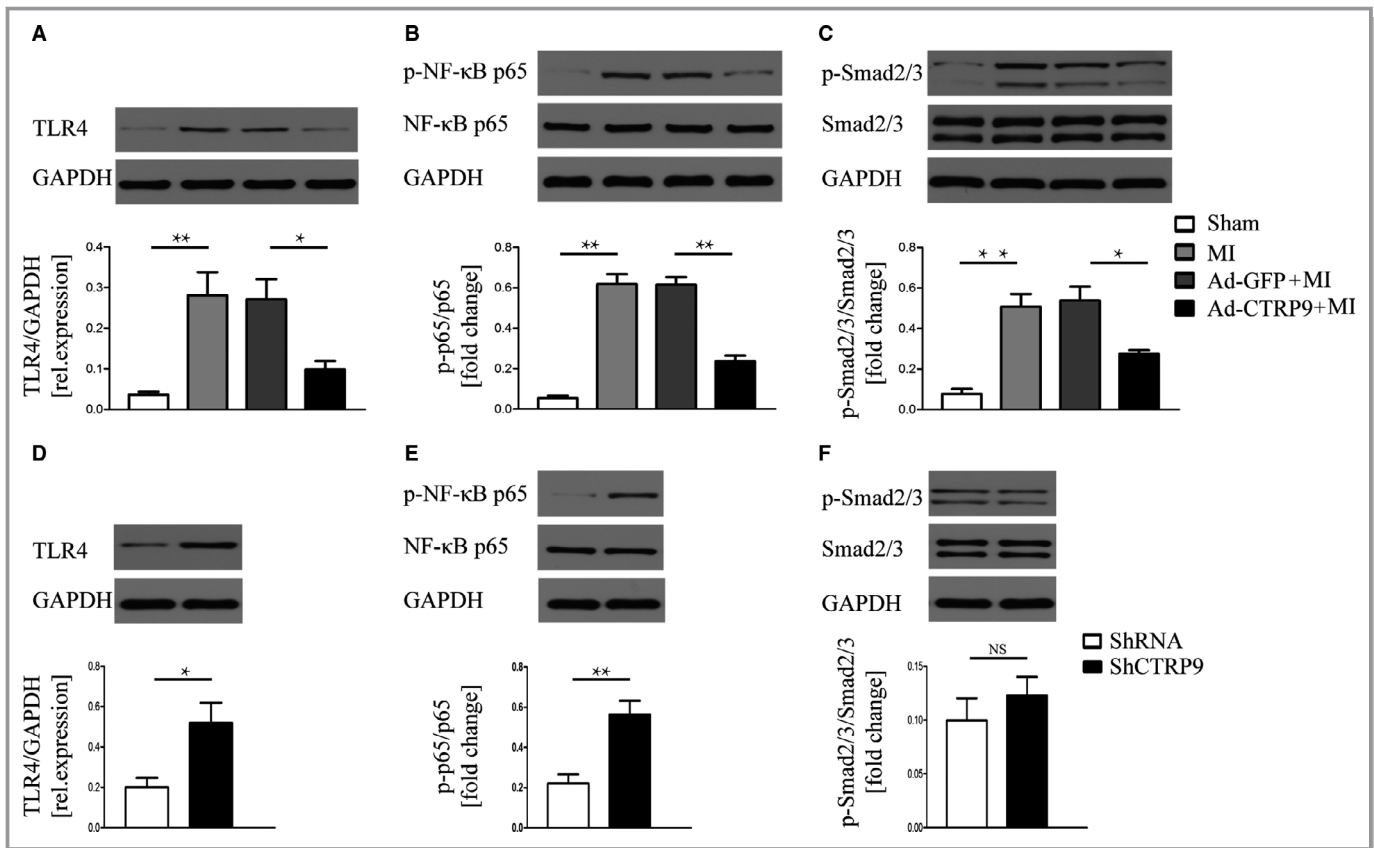


Figure 8. Effects of CTRP9 on expression of the Toll-like receptor 4/nuclear factor- κ B and Smad2/3 signaling pathways. Representative image for western blotting and protein expression levels of inflammatory markers Toll-like receptors 4, p-nuclear factor- κ B p65/nuclear factor- κ B p65 at 3 days post-myocardial infarction (**A** and **B**) and fibrosis markers p-Smad2/3/Smad2/3 at 7 days post-myocardial infarction (**C**). **D** through **F**, Alteration of atrial protein levels of Toll-like receptors 4, p-nuclear factor- κ B p65/nuclear factor- κ B p65 and p-Smad2/3/Smad2/3 under shRNA and shCTR99-treated rats. The data are expressed as the mean \pm SEM (n=4 per group). NS, $P>0.05$, $*P<0.05$, $**P<0.01$, the connection represents a comparison between the 2 groups. Ad-CTRP9 indicates adenoviral CTRP9 constitutively overexpression; Ad-GFP, adenovirus-encoding green fluorescent protein; MI, myocardial infarction; TLR4, Toll-like receptor 4; NF- κ B, nuclear factor-kappa B; p, phosphorylation.

persistent and permanent AF. Downregulation of CTRP9 resulted in atrial fibrosis, similar finding observed from a previous study that adiponectin knockout can promote cardiac fibrosis in mice.⁵⁷ However, a recent study reported that CTRP9 can promote cardiac hypertrophy and dysfunction in transverse aortic constriction,¹⁴ and showed a diverse CTRP9 effects that were different from our study. The different disease models may be a suitable explanation for the difference. Pathologically increased endogenous CTRP9 levels in transverse aortic constriction are possibly harmful, whereas decreased CTRP9 levels in MI have a protective effect. Mechanistically, although the silencing CTRP9 did not change the expression of smad2/3 phosphorylation, CTRP9 significantly attenuated MI-induced phosphorylation of Smad2/3 in LA tissues, suggesting that CTRP9 ameliorated atrial fibrosis at least partially by inactivating the Smad2/3 pathway in the MI disease model, thereby contributing to improving fibrosis-related arrhythmogenic substrates.

Inhibiting the atrial inflammation and fibrosis can effectively prevent AF susceptibility and IACT in different animal models, and the degree of atrial fibrosis inhibited is closely related to the duration of IACT shortened.^{20,28,58–60} Considering the proven effects of CTRP9 mentioned above, we conducted a correlation study and found that CTRP9 was negatively correlated with IL-1 β and AF duration, further proving that CTRP9 could reduce MI-caused higher vulnerability to AF, which suggests CTRP9 can inhibit AF occurrence partially by decreasing inflammation. Meanwhile, CTRP9 also shorten prolonged IACT after MI. Prolonged P-wave, which represented partial interatrial block, was chiefly caused by LA enlargement.²⁰ The duration of P wave had a slightly prolonged trend after MI in the present study, but there was no significant difference between the 4 groups. Inconsistent with previous results in the chronic phase post-MI,^{20,59} our findings measured lower incidence and duration of AF in the early phase post-MI, and undifferentiated P-wave duration may be attributed to shorter time in the MI model and

inapparently expanded atria. But, CTRP9 shortened PR interval at 7 days post-MI. Moreover, consistent with AERP in the long-term MI model, AERP was significantly prolonged in MI-induced rats in this study,⁶¹ whereas the specific mechanism of prolonging AERP in our MI model could not be elucidated in this study. Moreover, as a therapeutic purpose, CTRP9 did not notably reverse these effects. Indeed, compared with the long-term chronic MI model, our early phase of MI may also have some advantages which CTRP9 impacted AF occurrence, mainly focusing on atrial inflammation, interstitial fibrosis without markedly affecting AERP, independent of almost no expanded effect of LAD in the period. Surprisingly, we found that directed silence of CTRP9 can increase AF susceptibility, thereby avoiding the interference by affecting LV function, which further illustrated that CTRP9 itself is involved in the pathogenesis of AF.

We recognize that this study has some limitations. First, we have not identified the CTRP9 components that play a major role. Previous studies have demonstrated that the form of gCTRP9, but not fCTRP9, is the active cardioprotective isoform,^{17,62} while the adenoviral CTRP9 we constructed immediately expressed fCTRP9. However, considering that previous study suggest that cardiac tissue lysate has a strong ability to cleave fCTRP9 into gCTRP9.⁶³ Therefore, we can only infer that the active component after adenoviral transfection of CTRP9 into heart may still be gCTRP9, which needs to be further confirmed. Second, we do not have a thorough study on the specific mechanism of CTRP9 inhibiting atrial fibrosis and inflammation via corresponding cell experiment to verify it. Finally, Although AdCTRP9 and shCTRP9 treatment altered the expression of CTRP9 in rats, but not highly effective. The more exact clarification of the roles of CTRP9 on atrium, including more atrial structural remodeling, especially, electrical remodeling, will require a more specific and effective atrial-specific knockout/overexpression mouse model.

Conclusions

In general, the present study illustrated that CTRP9 could suppress atrial TLR4 elevation, p-NF- κ B p65, and p-Smad2/3 activation caused by MI, followed by promoting M2 macrophage polarization and inhibiting the production of fibrosis-related proteins, ameliorated cardiac function and decreased AF vulnerability. Meanwhile, downregulation of CTRP9 enhanced atrial inflammatory response, fibrosis and AF vulnerability. Therefore, CTRP9 could reduce arrhythmogenic substrate formation, subsequently decrease the occurrence of atrial arrhythmias post-MI.

Sources of Funding

This research was financially supported by the special fund for Technology Innovation of Hubei Province (Major Project) (No. 2016ACA153).

Disclosures

None.

References

- Pedersen OD, Abildstrom SZ, Ottesen MM, Rask-Madsen C, Bagger H, Kober L, Torp-Pedersen C, TRACE Study Investigators. Increased risk of sudden and non-sudden cardiovascular death in patients with atrial fibrillation/flutter following acute myocardial infarction. *Eur Heart J*. 2006;27:290–295.
- Romanov A, Martinek M, Purerfellner H, Chen S, De Melis M, Grazhdankin I, Ponomarev D, Losik D, Strelnikov A, Shabanov V, Karaskov A, Pokushalov E. Incidence of atrial fibrillation detected by continuous rhythm monitoring after acute myocardial infarction in patients with preserved left ventricular ejection fraction: results of the arrest study. *Europace*. 2018;20:263–270.
- Schmitt J, Duray G, Gersh BJ, Hohnloser SH. Atrial fibrillation in acute myocardial infarction: a systematic review of the incidence, clinical features and prognostic implications. *Eur Heart J*. 2009;30:1038–1045.
- Jabre P, Jouven X, Adnet F, Thabut G, Bielinski SJ, Weston SA, Roger VL. Atrial fibrillation and death after myocardial infarction: a community study. *Circulation*. 2011;123:2094–2100.
- Hwang HJ, Ha JW, Joung B, Choi EH, Kim J, Ahn MS, Lee MH, Jang Y, Chung N, Kim SS. Relation of inflammation and left atrial remodeling in atrial fibrillation occurring in early phase of acute myocardial infarction. *Int J Cardiol*. 2011;146:28–31.
- Galjautdinov GS, Gorelkin IV, Ibragimova KR, Sadriev RR. New-onset atrial fibrillation in settings of acute coronary syndrome. *Current issues. Ration Pharmacother*. 2018;14:451–457.
- Opincariu D, Chitu IM. Atrial fibrillation and acute myocardial infarction—an inflammation-mediated association. *Journal Of Cardiovascular Emergencies*. 2018;4:123–132.
- Dzeshka MS, Lip GY, Snezhitskiy V, Shantsila E. Cardiac fibrosis in patients with atrial fibrillation: mechanisms and clinical implications. *J Am Coll Cardiol*. 2015;66:943–959.
- Jalife J, Kaur K. Atrial remodeling, fibrosis, and atrial fibrillation. *Trends Cardiovasc Med*. 2015;25:475–484.
- Westman PC, Lipinski MJ, Luger D, Waksman R, Bonow RO, Wu E, Epstein SE. Inflammation as a driver of adverse left ventricular remodeling after acute myocardial infarction. *J Am Coll Cardiol*. 2016;67:2050–2060.
- Guo Y, Lip GY, Apostolakis S. Inflammation in atrial fibrillation. *J Am Coll Cardiol*. 2012;60:2263–2270.
- Friedrichs K, Klinke A, Baldus S. Inflammatory pathways underlying atrial fibrillation. *Trends Mol Med*. 2011;17:556–563.
- Nattel S. Molecular and cellular mechanisms of atrial fibrosis in atrial fibrillation. *JACC Clin Electrophysiol*. 2017;3:425–435.
- Appari M, Breitbart A, Brandes F, Szaroszyk M, Froese N, Korf-Klingebiel M, Mohammadi MM, Grund A, Scharf GM, Wang H, Zwadlo C, Fraccarollo D, Schrameck U, Nemer M, Wong GW, Katus HA, Wollert KC, Muller OJ, Bauersachs J, Heineke J. C1q-tnf-related protein-9 promotes cardiac hypertrophy and failure. *Circ Res*. 2017;120:66–77.
- Kambara T, Shibata R, Ohashi K, Matsuo K, Hiramatsu-Ito M, Enomoto T, Yuasa D, Ito M, Hayakawa S, Ogawa H, Aprahamian T, Walsh K, Murohara T, Ouchi N. C1q/tumor necrosis factor-related protein 9 protects against acute myocardial injury through an adiponectin receptor i-ampk-dependent mechanism. *Mol Cell Biol*. 2015;35:2173–2185.
- Sun Y, Yi W, Yuan Y, Lau WB, Yi D, Wang X, Wang Y, Su H, Wang X, Gao E, Koch WJ, Ma XL. C1q/tumor necrosis factor-related protein-9, a novel adipocyte-derived cytokine, attenuates adverse remodeling in the ischemic mouse heart via protein kinase a activation. *Circulation*. 2013;128:S113–S120.
- Su H, Yuan Y, Wang XM, Lau WB, Wang Y, Wang X, Gao E, Koch WJ, Ma XL. Inhibition of ctrp9, a novel and cardiac-abundantly expressed cell survival molecule, by tnfa-induced oxidative signaling contributes to exacerbated cardiac injury in diabetic mice. *Basic Res Cardiol*. 2013;108:315.
- Zhang P, Huang C, Li J, Li T, Guo H, Liu T, Li N, Zhu Q, Guo Y. Globular ctrp9 inhibits oxld-induced inflammatory response in raw 264.7 macrophages via ampk activation. *Mol Cell Biochem*. 2016;417:67–74.
- Prabhu SD, Frangogiannis NG. The biological basis for cardiac repair after myocardial infarction: from inflammation to fibrosis. *Circ Res*. 2016;119:91–112.
- Qiu H, Liu W, Lan T, Pan W, Chen X, Wu H, Xu D. Salvianolate reduces atrial fibrillation through suppressing atrial interstitial fibrosis by inhibiting TGF-beta1/Smad2/3 and TXNIP/NLRP3 inflammasome signaling pathways in post-MI rats. *Phytomedicine*. 2018;51:255–265.

21. Liu Q, Zhang H, Lin J, Zhang R, Chen S, Liu W, Sun M, Du W, Hou J, Yu B. C1q/TNF-related protein 9 inhibits the cholesterol-induced vascular smooth muscle cell phenotype switch and cell dysfunction by activating amp-dependent kinase. *J Cell Mol Med*. 2017;21:2823–2836.
22. Liu M, Yin L, Li W, Hu J, Wang H, Ye B, Tang Y, Huang C. C1q/TNF-related protein-9 promotes macrophage polarization and improves cardiac dysfunction after myocardial infarction. *J Cell Physiol*. 2019;234:18731–18747.
23. Yuan MJ, Wang T, Kong B, Wang X, Huang CX, Wang D. GHSR-1a is a novel pro-angiogenic and anti-remodeling target in rats after myocardial infarction. *Eur J Pharmacol*. 2016;788:218–225.
24. Yang M, Xiong J, Zou Q, Wang DD, Huang CX. Chrysin attenuates interstitial fibrosis and improves cardiac function in a rat model of acute myocardial infarction. *J Mol Histol*. 2018;49:555–565.
25. Liu M, Xu X, Zhao J, Tang Y. Naringenin inhibits transforming growth factor-beta1-induced cardiac fibroblast proliferation and collagen synthesis via G0/G1 arrest. *Exp Ther Med*. 2017;14:4425–4430.
26. Glukhov AV, Kalyanasundaram A, Lou Q, Hage LT, Hansen BJ, Belevych AE, Mohler PJ, Knollmann BC, Periasamy M, Gyorke S, Fedorov VV. Calsequestrin 2 deletion causes sinoatrial node dysfunction and atrial arrhythmias associated with altered sarcoplasmic reticulum calcium cycling and degenerative fibrosis within the mouse atrial pacemaker complex. *Eur Heart J*. 2015;36:686.
27. Hayashi H, Wang C, Miyauchi Y, Omichi C, Pak HN, Zhou S, Ohara T, Mandel WJ, Lin SF, Fishbein MC, Chen PS, Karagueuzian HS. Aging-related increase to inducible atrial fibrillation in the rat model. *J Cardiovasc Electrophysiol*. 2002;13:801–808.
28. Kondo H, Takahashi N, Gotoh K, Fukui A, Saito S, Aoki K, Kume O, Shinohara T, Teshima Y, Saikawa T. Splenectomy exacerbates atrial inflammatory fibrosis and vulnerability to atrial fibrillation induced by pressure overload in rats: possible role of spleen-derived interleukin-10. *Heart Rhythm*. 2016;13:241–250.
29. Lee TM, Chang NC, Lin SZ. Dapagliflozin, a selective sglT2 inhibitor, attenuated cardiac fibrosis by regulating the macrophage polarization via stat3 signaling in infarcted rat hearts. *Free Radic Biol Med*. 2017;104:298–310.
30. Xu J, Cui G, Esmailian F, Plunkett M, Marelli D, Ardehali A, Odum J, Laks H, Sen L. Atrial extracellular matrix remodeling and the maintenance of atrial fibrillation. *Circulation*. 2004;109:363–368.
31. Bezerra OC, Franca CM, Rocha JA, Neves GA, Souza PRM, Teixeira Gomes M, Malfitano C, Loleiro TCA, Dourado PM, Llesuy S, de Angelis K, Irigoyen MCC, Ulloa L, Consolim-Colombo FM. Cholinergic stimulation improves oxidative stress and inflammation in experimental myocardial infarction. *Sci Rep*. 2017;7:13687.
32. Burstein B, Maguy A, Clement R, Gosselin H, Poulin F, Ethier N, Tardif JC, Hebert TE, Calderone A, Nattel S. Effects of resveratrol (trans-3,5,4'-trihydroxystilbene) treatment on cardiac remodeling following myocardial infarction. *J Pharmacol Exp Ther*. 2007;323:916–923.
33. Bozkurt E, Arslan S, Acikel M, Erol MK, Gurlertop Y, Yilmaz M, Koca H, Atesal S. Left atrial remodeling in acute anterior myocardial infarction. *Echocardiography*. 2007;24:243–251.
34. Hu YF, Chen YJ, Lin YJ, Chen SA. Inflammation and the pathogenesis of atrial fibrillation. *Nat Rev Cardiol*. 2015;12:230–243.
35. Sun Z, Zhou D, Xie X, Wang S, Wang Z, Zhao W, Xu H, Zheng L. Cross-talk between macrophages and atrial myocytes in atrial fibrillation. *Basic Res Cardiol*. 2016;111:63.
36. Francis Stuart SD, De Jesus NM, Lindsey ML, Ripplinger CM. The crossroads of inflammation, fibrosis, and arrhythmia following myocardial infarction. *J Mol Cell Cardiol*. 2016;91:114–122.
37. Begieneman MP, Emmens RW, Rijvers L, Woudstra L, Paulus WJ, Kubat B, Vonk AB, van Rossum AC, Wouters D, Zeerleder S, van Ham M, Schalkwijk CG, Niessen HW, Krijnen PA. Myocardial infarction induces atrial inflammation that can be prevented by C1-esterase inhibitor. *J Clin Pathol*. 2016;69:1093–1099.
38. Ben-Mordechai T, Palevski D, Glucksam-Galnoy Y, Elron-Gross I, Margalit R, Leor J. Targeting macrophage subsets for infarct repair. *J Cardiovasc Pharmacol Ther*. 2015;20:36–51.
39. Frangogiannis NG. The mechanistic basis of infarct healing. *Antioxid Redox Signal*. 2006;8:1907–1939.
40. Cheng Y, Rong J. Macrophage polarization as a therapeutic target in myocardial infarction. *Curr Drug Targets*. 2018;19:651–662.
41. Shirakawa K, Endo J, Kataoka M, Katsumata Y, Yoshida N, Yamamoto T, Isobe S, Moriyama H, Goto S, Kitakata H, Hiraide T, Fukuda K, Sano M. IL (interleukin)-10-STAT3-Galectin-3 axis is essential for osteopontin-producing reparative macrophage polarization after myocardial infarction. *Circulation*. 2018;138:2021–2035.
42. Jung M, Ma Y, Iyer RP, DeLeon-Pennell KY, Yabluchanskiy A, Garrett MR, Lindsey ML. IL-10 improves cardiac remodeling after myocardial infarction by stimulating M2 macrophage polarization and fibroblast activation. *Basic Res Cardiol*. 2017;112:33.
43. Gombozhapova A, Rogovskaya Y, Shurupov V, Rebenkova M, Kzhyshkowska J, Popov SV, Karpov RS, Ryabov V. Macrophage activation and polarization in post-infarction cardiac remodeling. *J Biomed Sci*. 2017;24:13.
44. Zhou D, Yang K, Chen L, Wang Y, Zhang W, Xu Z, Zuo J, Jiang H, Luan J. Macrophage polarization and function: new prospects for fibrotic disease. *Immunol Cell Biol*. 2017;95:864–869.
45. Yang N, Cheng W, Hu H, Xue M, Li X, Wang Y, Xuan Y, Li X, Yin J, Shi Y, Yan S. Atorvastatin attenuates sympathetic hyperinnervation together with the augmentation of M2 macrophages in rats postmyocardial infarction. *Cardiovasc Ther*. 2016;34:234–244.
46. Wen ZF, Liu HX, Gao R, Zhou M, Ma J, Zhang Y, Zhao JJ, Chen YQ, Zhang TY, Huang F, Pan N, Zhang JP, Fox BA, Hu HM, Wang LX. Tumor cell-released autophagosomes (TRAPS) promote immunosuppression through induction of M2-like macrophages with increased expression of PD-L1. *J Immunother Cancer*. 2018;6:151.
47. Oeckinghaus A, Hayden MS, Ghosh S. Crosstalk in NF-kappaB signaling pathways. *Nat Immunol*. 2011;12:695–708.
48. Zhang P, Shao L, Ma J. Toll-like receptors 2 and 4 predict new-onset atrial fibrillation in acute myocardial infarction patients. *Int Heart J*. 2018;59:64–70.
49. Mandal P, Roychowdhury S, Park PH, Pratt BT, Roger T, Nagy LE. Adiponectin and heme oxygenase-1 suppress TLR4/MyD88-independent signaling in rat Kupffer cells and in mice after chronic ethanol exposure. *J Immunol*. 2010;185:4928–4937.
50. Saito S, Teshima Y, Fukui A, Kondo H, Nishio S, Nakagawa M, Saikawa T, Takahashi N. Glucose fluctuations increase the incidence of atrial fibrillation in diabetic rats. *Cardiovasc Res*. 2014;104:5–14.
51. Fukui A, Takahashi N, Nakada C, Masaki T, Kume O, Shinohara T, Teshima Y, Hara M, Saikawa T. Role of leptin signaling in the pathogenesis of angiotensin II-mediated atrial fibrosis and fibrillation. *Circ Arrhythm Electrophysiol*. 2013;6:402–409.
52. Harada M, Van Wagoner DR, Nattel S. Role of inflammation in atrial fibrillation pathophysiology and management. *Circ J*. 2015;79:495–502.
53. Everett TH, Olgin JE. Atrial fibrosis and the mechanisms of atrial fibrillation. *Heart Rhythm*. 2007;4:S24–S27.
54. Rahmutula D, Marcus GM, Wilson EE, Ding CH, Xiao Y, Paquet AC, Barbeau R, Barczak AJ, Erle DJ, Olgin JE. Molecular basis of selective atrial fibrosis due to overexpression of transforming growth factor-beta1. *Cardiovasc Res*. 2013;99:769–779.
55. Nattel S, Burstein B, Dobrev D. Atrial remodeling and atrial fibrillation: mechanisms and implications. *Circ Arrhythm Electrophysiol*. 2008;1:62–73.
56. Heijman J, Voigt N, Nattel S, Dobrev D. Cellular and molecular electrophysiology of atrial fibrillation initiation, maintenance, and progression. *Circ Res*. 2014;114:1483–1499.
57. Fujita K, Maeda N, Sonoda M, Ohashi K, Hibuse T, Nishizawa H, Nishida M, Hiuge A, Kurata A, Kihara S, Shimomura I, Funahashi T. Adiponectin protects against angiotensin II-induced cardiac fibrosis through activation of PPAR-alpha. *Arterioscler Thromb Vasc Biol*. 2008;28:863–870.
58. Kume O, Takahashi N, Wakisaka O, Nagano-Torigoe Y, Teshima Y, Nakagawa M, Yufu K, Hara M, Saikawa T, Yoshimatsu H. Pioglitazone attenuates inflammatory atrial fibrosis and vulnerability to atrial fibrillation induced by pressure overload in rats. *Heart Rhythm*. 2011;8:278–285.
59. Ma J, Yin C, Ma S, Qiu H, Zheng C, Chen Q, Ding C, Lv W. Shensong yangxin capsule reduces atrial fibrillation susceptibility by inhibiting atrial fibrosis in rats with post-myocardial infarction heart failure. *Drug Des Devel Ther*. 2018;12:3407–3418.
60. Huang Z, Chen XJ, Qian C, Dong Q, Ding D, Wu QF, Li J, Wang HF, Li WH, Xie Q, Cheng X, Zhao N, Du YM, Liao YH. Signal transducer and activator of transcription 3/microRNA-21 feedback loop contributes to atrial fibrillation by promoting atrial fibrosis in a rat sterile pericarditis model. *Circ Arrhythm Electrophysiol*. 2016;9:e003396.
61. Zhang Y, Dedkov EI, Lee B III, Li Y, Pun K, Gerdes AM. Thyroid hormone replacement therapy attenuates atrial remodeling and reduces atrial fibrillation inducibility in a rat myocardial infarction-heart failure model. *J Card Fail*. 2014;20:1012–1019.
62. Yan WJ, Guo YZ, Tao L, Lau WB, Gan L, Yan ZY, Guo R, Gao EH, Wong GW, Koch WL, Wang YJ, Ma XL. C1q/tumor necrosis factor-related protein-9 regulates the fate of implanted mesenchymal stem cells and mobilizes their protective effects against ischemic heart injury via multiple novel signaling pathways. *Circulation*. 2017;136:2162–2177.
63. Yuan Y, Lau WB, Su H, Sun Y, Yi W, Du Y, Christopher T, Lopez B, Wang Y, Ma XL. C1q-TNF-related protein-9, a novel cardioprotective cardiokine, requires proteolytic cleavage to generate a biologically active globular domain isoform. *Am J Physiol Endocrinol Metab*. 2015;308:E891–E898.